

Hydrogeological and Groundwater Investigations of Niksar Basin, Tokat, Turkey

Syed Mobasher Aftab^{1*}

¹Balochistan University of Information Technology, Engineering & Management Sciences, Quetta

*Corresponding author's email: syed.aftab@live.com

Submitted date: 03/06/2020 Accepted date: 24/02/2021 Published online: 31/03/2021

Abstract

The study area comprises the Niksar Basin of Tokat district, located in the Middle Black Sea region, Turkey. The Kelkit River flows through the center of Niksar Valley. The lithological units exposed on the northern and southern parts of Kelkit River have disparate geological sequences; grouped as "Pontid" and "Anatolit" respectively. The micritic and biomicritic limestone of Upper Jurassic - Lower Cretaceous, limestone of Upper Cretaceous, and the detrital limestone of Upper Cretaceous - Lower Paleocene form characteristic karstic aquifers. In the valley, a thick sequence of loose gravel, sand, and clayey materials of Pliocene and Quaternary are deposited. The presence of clay lenses in these materials created suitable hydrodynamic conditions for the formation of confined and unconfined aquifers. The karstic aquifers recharged through precipitation and valley-fill aquifer through Kelkit River. These aquifers fulfill the water supply demands of the entire population of Niksar Town and surrounding villages. This paper summarizes hydrogeological research conducted on all basinal formations. The Karstic aquifers and the unconfined aquifer of valley-fill sediments were systematically analyzed. The physical characteristics of the aquifer formations, karstification, occurrence, and movement of groundwater, recharge, and discharge sources, and discharge hydrograph analysis were conducted. The exposed hydrogeological formations were recharged through precipitation by $0.329 \times 10^9 \text{ m}^3$ and discharged by $0.317 \times 10^9 \text{ m}^3$ during the study period. The karstic formations were recharged from precipitation by $45.0 \times 10^6 \text{ m}^3$, while discharged from karstic springs by $47.88 \times 10^6 \text{ m}^3$ of water. The discharge rate of major karstic spring ranges from 4.3 to 430 l/s and the discharge coefficient ranges from 0.004-0.026 day⁻¹. The storage capacity of springs varies from $0.14-5.01 \times 10^6 \text{ m}^3$ and the total discharged volume during the study period was $48.10 \times 10^6 \text{ m}^3$. The groundwater budget of the valley-fill aquifer represents that during the study period recharged from different sources $0.266 \times 10^9 \text{ m}^3$ and discharged $0.263 \times 10^9 \text{ m}^3$ by all sources. The conceptual hydrogeological model of Niksar Valley simulates geological, hydroclimatic, hydrogeomorphologic, hydrostratigraphic, hydrogeological, and hydrologic field environments.

Keywords: Pontid, Anatolit, Karstic aquifer, Niksar Basin, Turkey.

1. Introduction

The Niksar Basin is selected to estimate the groundwater budget and investigate hydrogeological features in this region. The area is geographically situated between $36^{\circ}43'50''$ – $37^{\circ}10'25''$ East Longitude and $40^{\circ}28'25''$ – $40^{\circ}41'50''$ North Latitude, as shown in Figure 1. The geological, hydrogeological, and groundwater investigations conducted on the basin spread over an area of 655 km². The investigations are part of the Ph.D. dissertation submitted to the Department of Geological Engineering, Faculty of Engineering, Ankara University, Turkey, (Aftab, 1989). The groundwater budget was estimated for the valley aquifer that covers an area of 141 km². The Niksar Basin has a diverse geological and

tectonic setup with complicated aquifer systems ranging from confined to unconfined and from hard-rocks to karstic aquifers. Substantial efforts were made to estimate the hydrogeological framework characterization and groundwater investigations of all hydrostratigraphic units. The exposed geological formations of similar hydrogeological characteristics are qualitatively grouped as permeable, semi-permeable, and impermeable units. Two impermeable units comprised of schists, marl, and mudstones. Three semipermeable units comprised of conglomerate, sandstone, limestone with other intercalations. Two separate karstified limestone units studied separately as Lower and Upper Karstic Units. The karstification processes, recharge, and

discharge through karstic springs were evaluated. The groundwater flow in different lithological units has directional anisotropic behavior because of primary sedimentary, igneous, and metamorphic features, geological structures, and hydrologic properties. The study comprises geological and hydrogeological factors affecting the vertical and horizontal distribution of groundwater. Inventory and periodical monitoring of all surface and groundwater resources were carried out. The recharge and discharge zones of aquifers were evaluated, precipitation, surface and groundwater interaction, and groundwater fluctuations assessed. The fifty-two groundwater springs having discharge more than 1.0 l/s were periodically monitored. The recession curve analysis and reserve estimation of 9 major karstic springs were calculated. The well-pumping and injection field tests have been performed. Groundwater table and piezometric surface and equal variation maps were prepared. The groundwater budgets of the Quaternary aquifer covering the valley floor were appraised.

2. Hydroclimatology

The twenty-year average precipitation amount of the study area is 547mm. The maximum precipitation of 164.5mm falls in October and a minimum of 0.7mm in

September. To calculate the precipitation during the study period Thiessen Polygon and Isohyetal Precipitation maps were prepared with data of seven existing and two new meteorological stations established in the Niksar Basin. The cumulative yearly precipitation for the study area is 555mm. Precipitation for the budget period is 580mm and 571mm with Isohyetal and Polygon Methods respectively, the average of both methods is 576mm. The twenty-year averages minimum and maximum temperature of the study area ranges from 4.4-23.5°C in January and July respectively. The climogram of the study area based on twenty year's temperatures and precipitation values represent January and December are the rainy months. February to May and October-November are transitional, while June-September are dry months. The De Martonne's (1942) aridity index (I) of 12.87 represents that the study area embraced half-dry to wet-weather. The climogram of the study area is presented in Figure 2a. The climatic pattern of the area may represent as C1 B2' S b'4, accordingly characterize as dry-less-humid (C1), mesothermal (B2'), excess-water in winter at mild-level (S), and near to areas effected by sea (b'4). The average humidity value of the last twenty years is 55.3%. The minimum humidity was 52% in March 1988 and a maximum of 74% in December 1989.

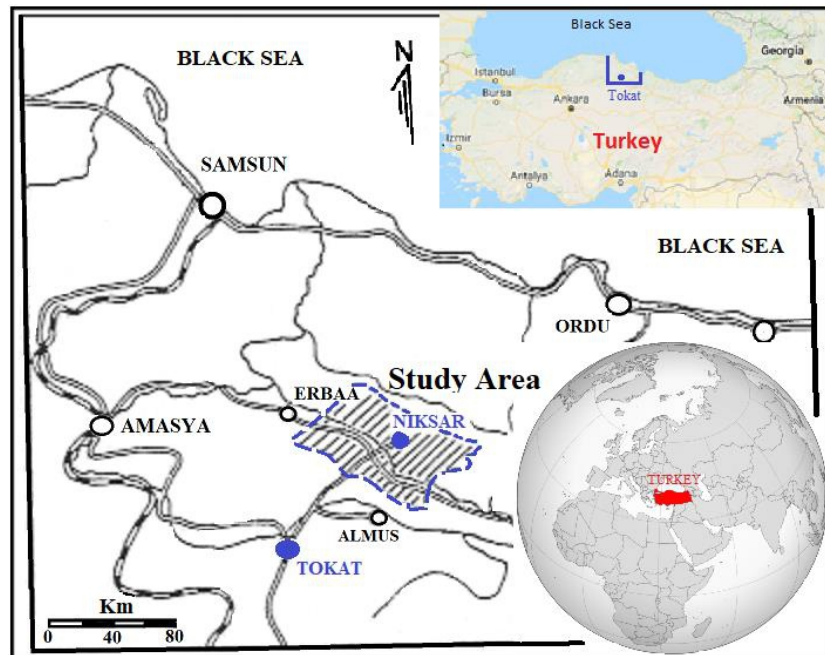


Fig. 1. Location map of the study area.

Turc's method utilized to calculate yearly Etr which is 472mm and 86% of precipitation (Turc, 1961). For the groundwater budget, the excess soil-water is 100%. Thornthwaite's (1948) climatic water balance model utilized meteorological data to estimate monthly potential evapotranspiration (Etpc) and computes actual evapotranspiration (Etr) and monthly surface runoff. Precipitation and potential evapotranspiration graph have been prepared for the groundwater budget period from October 1986 to September 1987, Figure 2b. The graph representing, the periods of water surplus and deficit, soil moisture utilizing, and

soil moisture recharging. The Etpc was 742mm, Etr 357mm, total precipitation 551mm, water deficit 384mm, and water surplus 194mm. Consequently, during the budget period, 65% of the total precipitation becomes part of the atmosphere through evapotranspiration. The soil moisture recharge during the same period was up to 35% of precipitation. The groundwater percolation and surface runoff are 35% of the precipitation. The soil water budget of the area is presented in Table 1.

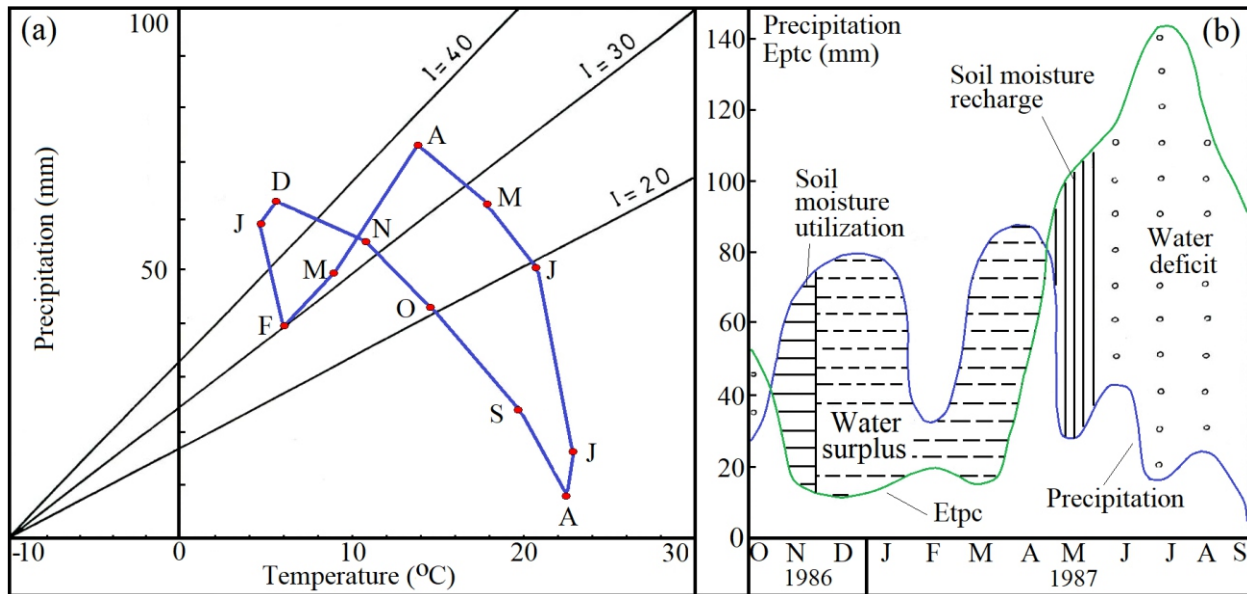


Fig. 2. a) The climogram of study area based on twenty years average values, b) Precipitation and potential evapotranspiration graph, October 1986 to September 1987.

Table 1. The soil water budget of Niksar Basin.

Budget Elements	Oct	Nov	Dec	Jan	Feb	Mar	Apr	May	Jun	Jul	Aug	Sep	Total
Monthly Temp. $^{\circ}\text{C}$	14.2	6.7	5.4	6.1	7.6	5.3	11.5	18.7	20.4	23.5	21.3	19.1	-
Precipitation (mm)	26.5	66.7	78.4	77.9	32.5	73.5	87.0	27.8	41.6	15.6	23.4	0.0	550.9
Thermal Index (I)	4.9	1.6	1.1	1.4	1.9	1.1	3.5	7.4	8.4	10.4	9.0	7.6	58.2
Latitude Correction Factor (40° - 35°)	1.0	0.8	0.8	0.8	0.8	1.0	1.1	1.2	1.3	1.3	1.2	1.0	-
Etp (mm)	55.8	19.5	14.4	17.1	23.3	14.1	41.6	82.1	92.7	113.0	98.5	84.6	656.7
Etr (mm)	26.5	16.2	11.7	14.4	19.3	14.5	46.1	101.8	67.6	15.6	23.4	0.0	357.1
Etpc (mm)	53.6	16.9	11.7	14.4	19.3	14.5	46.1	101.8	115.9	143.6	116.2	88.0	741.9
Water utilization (mm)	0.0	50.5	100	100	100	100	100	26.0	0.0	0.0	0.0	0.0	-
Water surplus (mm)	0.0	0.0	17.2	63.5	13.2	59.0	40.9	0.0	0.0	0.0	0.0	0.0	193.9
Water deficit (mm)	27.1	0.0	0.0	0.0	0.0	0.0	0.0	0.0	48.3	128.0	92.8	88.0	384.2
Runoff (mm)	0.0	0.0	8.6	36.1	24.6	41.8	41.4	0.0	0.0	0.0	0.0	0.0	152.5

3. Hydrogeomorphology

The topography of the valley varies between 250-400m from NW-SE parallel to the flow direction of the Kelkit River. The topographic slope of the valley is about 2%, the surrounding mountains are cut by streams with a slope range from 2-15%. The basin-low is 250masl toward the western side of the valley and the highest Kocatepe Mountain (M) 1,822masl in the NE. The hypsometric curve represents the average topographic height of the basin is 700masl. The oro-hydrographic map of the basin prepared to demarcate ridges; drainage pattern, precipitation area, and water divide lines with topographic maps, 1/25,000. In the eastern part, the ridges extended from E-W following the tectonic pattern of the region, Seymen (1975). The prominent ridges are Taslica, Karacal M 1,808, and Alacal M 1,811masl. These ridges developed in Upper Jurassic-Lower Cretaceous limestone formations and form the water divide of Canakci Stream (S). The northern slopes extended N-S, developed in the Jurassic and Eocene rocks, Golaga 1,502masl, is the highest ridges. The southern slopes extended in E-W and were composed of metamorphic rocks of the Jurassic - Eocene. Starting from west Kocadagi M 815, and Sumbulu M 1,011masl are prominent ridges.

The mountains surrounding the Niksar Basin are covered with forests which are around 53% of the landmass of the basin. The entire basinal plain is irrigated with the Kelkit River. The hydrography represents that structure, lithology, vegetation cover, and soil type affect the development of drainage pattern. Kelkit River flows in the center of the valley from S-N, while all other streams flow towards the Kelkit River. The Canakci S is the biggest stream passing through Niksar Town from E-W. The floor of the stream is deep and narrow and developed along Ladik-Niksar-Bereketli Fault Zone, flows in magmatic rocks of the Eocene. The drainage pattern of the associated streams is rectangular and dendritic in nature. Toward SW of Niksar, the Aybellini and Aksu Streams, follow the Hanyeri-Gokcебet Fault Zone and flows from E-W. The valleys are narrow, V-shaped and the drainage patterns of associated streams are dendritic and rectangular. The

shallow and rectangular drainage pattern is developed in areas where karstic rocks are exposed. The gradient of prominent streams, estimated with base profiles, accordingly based on the change in gradient streams was divided into the lower, middle, and upper parts.

The average temperature, precipitation, and Kelkit River flow hydrographs of the last twenty-year values have been prepared for correlation. The average precipitation and Kelkit River flow values have a direct relationship. In April, the cumulative maximum precipitation was 39.6mm and the maximum flow was 263.3m³/s, Figure 3. Similarly, in August, the minimum precipitation was 7.8mm accordingly flow drops to the minimum level of 13.3m³/s. The daily average flow values of the Kelkit River were utilized to calculate the base flow during the study period. The flow hydrographs of daily total precipitation and daily average flows were prepared to evaluate the relationship between flow and floods. Schoeller's Hydrographical Method was utilized to estimate the surface flow separated from the base flow (Schoeller, 1962). Thereafter, the surface and groundwater flow of each area were analyzed. During the study period, the Kelkit River flow to the basin was 5.57×10^9 m³ and the base flow was 3.12×10^6 m³. The flooding in the Kelkit River occurred from March to June. The highest instantaneous flood of 905m³/s at Fatli Bridge was observed on April 16, 1968, and during the study, period 654m³/s on April 13, 1987, (General Directorate of Electrical Affairs Etud Administration of Turkey, EIE, 1968-1988). The precipitation area of Canakci S is 93.8km², the discharge measurements were conducted 2-3 times per month at Kirec Bridge. The maximum flow of 1.94×10^3 m³/s was observed on April 15, 1987, and a minimum of 0.13m³/s on August 25, 1986. The cumulative yearly surface flow of Canakci S was 35.82×10^6 m³ and the base flow was 11.48×10^6 m³. In central part of the Niksar Valley, the groundwater table is 0-2m deep in an area of about 50 km². General Directorate of State Hydraulic Works of Turkey (DSI) maintaining a drainage system of two-meter-deep to control the water table, (General Directorate of State Hydraulic Works of Turkey, 1968-1988). The drainage system having main and subsidiary surface drainage

canals. The water level fluctuates in the drainage canals have a similar pattern related to the water level of Kelkit River. The minimum and maximum discharge from drainage canals was 3.21 and 6.15m³/s observed on October 2, 1986, and October 13, 1987, respectively. The

cumulative total discharge from drainage canals for the budget period was 129.9x106m³. The surface and groundwater interaction through the hydrographic relationship between precipitation, streamflow, and groundwater levels are presented in Figure 3.

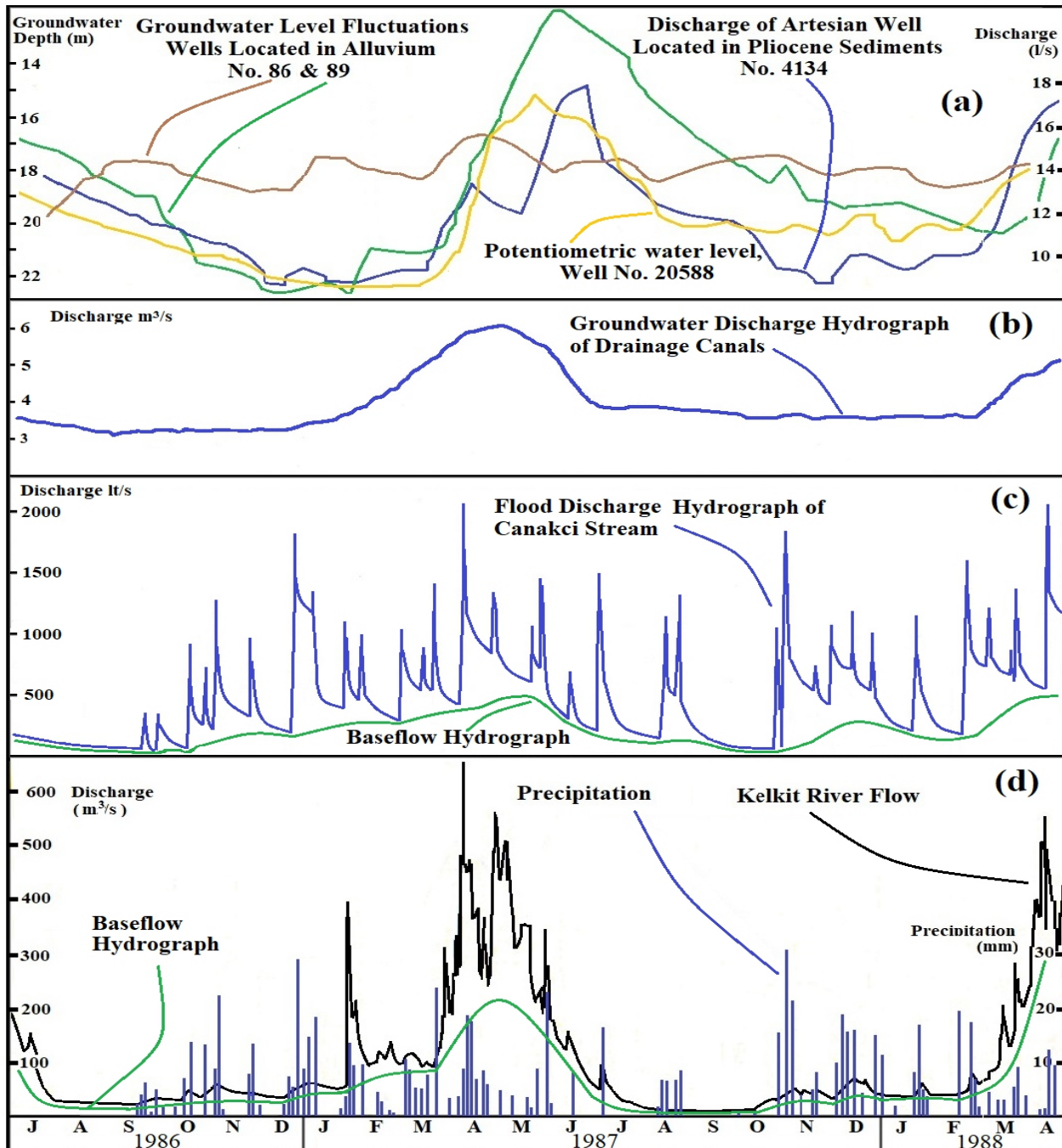


Fig. 3. Surface and groundwater interactions: a) groundwater level fluctuations of the unconfined aquifer, discharge of artesian well and piezometric water levels, b) groundwater discharge of drainage canals, c) flood and base flow discharge of Canakci Stream, d) precipitation and flow of Kelkit River.

4. Hydrogeology

The Niksar Valley developed as a huge tectonic depression, along the Kelkit River. The lithological units exposed on the northern and southern parts of the Kelkit River are grouped as "Pontid" and "Anatolid" respectively, (Blumenthal, 1950). These two groups of rocks are studied separately and are separated from each other along the Kelkit River towards the east of the valley. The Pontid Group is composed of eleven lithological formations and age-wise ranges from Paleozoic to Quaternary. The Anatolit Group is divided into four formations ranges from Paleozoic to Cenozoic. The Paleozoic metamorphic rocks form the basement in both groups, at Anatolid these rocks are exposed on a huge area while comparatively cover a small area at Pontid. At Pontid on metamorphic schists due to tectonic activities of the Lower Jurassic a sedimentary succession of sandstone, conglomerate, and synsedimentary volcanics were deposited. The limestone of the Upper Jurassic - Lower Cretaceous deposited above the succession. During Upper Cretaceous, the clayey limestone with andesitic tuff deposited. The marl and mudstone deposited in Upper Maastrichtian and the detrital limestone deposited during the Upper Maastrichtian - Lower Palaeocene. The flysch unconformably deposited in Lower Lutetian over the older formations. The Upper Lutetian andesitic and basaltic rocks cover the flysch. At Anatolid, the Palaeozoic schists thrust over the Cretaceous Ophiolitic Series at the south of Niksar. The flysch of Lower Lutetian deposited unconformably over the ophiolites and during Upper Lutetian volcanic breccia covered all the older formations. The exposed lithological and stratigraphic units have different hydrogeological characteristics. The formations of similar hydrogeological characteristics are qualitatively grouped as permeable, semi-permeable, and impermeable formations.

Semipermeable Unit (AG-2) is composed of limestone of Lutetian and thin-bedded mudstone, volcanogenic sandstone, and interbedded conglomerate lenses. The volcanic andesitic and basaltic lava flows, tuff, and agglomerate of Upper Lutecian are impermeable but secondary permeability is

well developed. These rocks are exposed and seen over a large area in the northeastern part of the hydrogeological map. The Impermeable Basement is comprised of metamorphic series of Paleozoic, composed of schists, metaagglomerate, metachert, and metatuff. The schists are impermeable, hydraulic conductivity developed in marbles, metaagglomerate, and metatuffs. The southwestern part of the hydrogeological map is covered mostly with Semipermeable Unit (AG-3) and Impermeable Basement (GST). The Semipermeable unit started with shale of Lower Lutecian, interbedded with sandstone, conglomerate, and micritic limestone. Sandstone, conglomerate, and limestone units have well-developed fracture systems. The upper layers are composed of volcanic breccia of Upper Lutecian along-with andesitic lava flows. The hydrogeological map and stratigraphic column of the basin prepared based on similar hydrogeological and hydrostratigraphic parameters are presented in Figures 4 and 5 respectively.

Hydrostratigraphy is related to the identification of rock units, lithological disparities, hydrogeological properties, geomorphology, and structural and tectonic setups. Geologically exposed geological units comprised of clay, sand, gravel, conglomerate, marl, shale, mudstone, sandstone, limestone, along-with many varieties of igneous and metamorphic rocks. Altogether, geologically fourteen diverse lithological units hydrogeologically assembled into ten units Figure 4, and hydrostratigraphically into eight groups, see Figure 5. The analysis is associated with the identification of potential groundwater bearing zones, recharge and discharge ranges, evapotranspiration, surface, and groundwater interaction zones, and fluctuation in reserve estimations related to hydrostratigraphy. The description of the lithological and hydrostratigraphic units are presented in the following paragraphs.

4.1. Impermeable Basement (GST)

The metamorphic series of Paleozoic forms the basement, which is composed of schists with the intercalations of metaagglomerate, metachert, and metatuff. The

marbles are exposed in the form of islands in the schists. Schists are impermeable while the secondary porosity and permeability developed in metaagglomerate, metatuffs, and marbles. A few springs with discharge, vary from 0.2 to 1.0 L/s observed from metaagglomerate, metatuff, and marble formations. The marble is badly fractured and exposed in the form of small blocks and has a good aquifer characteristic. Because of the limited exposure and recharging area, the discharges took place from a few small springs. Precipitation is the only source of recharge of the formation, the coefficient of recharge varies from estimated as 1-2%. The narrow and deep dendritic drainage system indicates greater surface runoff.

4.2. Semipermeable Unit (AG-1)

The Jurassic rocks are composed of conglomerate, sandstone; lava flows, tuff, marl, and mudstone which are overlying the basement rocks. The conglomerate is composed of volcanic pebbles and boulders which are semi-rounded and poorly sorted. Sandstone is large-grained and poorly sorted. Marl is hard and highly jointed and fractured while mudstone is thin-bedded. At places in this sedimentary series, lava flow is exposed. All units are well jointed, fractured, and faulted structures. The precipitation is the only source of recharge through a large surface area. Recharge and discharge took place through secondary porosity and permeability. A few springs having discharge, vary from 0.3-1.0 L/s are present in the formation. The recharge percentage varies as per change in lithology of individual units. The estimated average coefficient of recharge for the Jurassic formation is 4%, which varies from low-high in places where clayey to sandy units are exposed respectively.

4.3. Permeable Lower Karstic Unit (GK-1)

The Jurassic to Cretaceous age limestone formations has a well-developed karstic system in the area. The lower units of formation range from Jurassic to Lower Cretaceous and are composed of necrotic, biomicritic, dymicritic, intrasparite, and detritic limestone. The upper units are of the Upper Cretaceous age and are composed of clayey-limestone interbedded

with marl and andesitic tuff. These limestones show a lithologic change from micritic to biomicritic and detritic origins. An interconnected diffused and conduit flow system developed together in both karstic limestone units, (Atkinson and Hydrol, 1977; and Gunn et al. 1985). Both units investigated as a single aquifer from groundwater movement, recharge, and discharge point of view. These limestone units have a well-developed karstic system. The hydrologic properties vary with the variation of lithology and mode of deposition. Despite all lithological variations, the secondary permeability is much greater than the primary. The groundwater movement varies with the variation of lithology and groundwater-bearing rock properties. The lateral extent of the recharge area is quite significant, and precipitation is the only source of recharge. The units discharge through several small to large karstic springs. Surface drainage is poorly developed. The infiltration rate has varied, from place to place depending upon structure, topography, soil cover, and solution cavities. The average value of the coefficient of permeability is 40%.

4.4. Impermeable Unit (GSB)

The Maastrichtian rocks form an impermeable unit, which is composed of thin-bedded marl and mudstone. The marl and mudstone are interbedded with thin bentonite layers and thick tuff of blocky structure. Precipitation is the only source of recharge with a considerably smaller area of recharge. The coefficient of recharge estimated as varies from 1-2 %t, no spring observed in this rock unit.

4.5. Permeable Upper Karstic Unit (GK-2)

This karstic unit is of the Upper Maastrichtian-Lower Paleocene age and is composed of detrital limestone. The limestone formation forms a separate karstic region of good aquifer characteristics. The exposed recharge area through precipitation is small and the estimated coefficient of recharge is 40%. The unit discharges its water from springs that emerge by the contacts with other geological formations.

4.6. Semipermeable Unit (AG-2)

The unit composed of limestone of Lutetian at the base and continues upward with thin-bedded mudstone, volcanogenic sandstone, and interbedded conglomerate lenses. Above these beds in the northern part of the study area volcanic andesitic and basaltic lava flows and tuff and agglomerate of Upper Lutecian age covered a large area. At places, this unit is covered by organic clays of varying thickness. The rock formations are impermeable but secondary permeability is well developed. The surface drainage follows the regional structure of the area. Many small and a few large springs are oozing out along the major fracture and fault systems. In the study area, thin basaltic dykes of Miocene age cut the volcanic and older formations. The basaltic rocks are exposed in the form of huge blocks with increased hydraulic conductivities. The famous excellent quality "Ayaz Spring" emerges from the basaltic formation. The precipitation is the only source of recharge to a large areal extent. The estimated coefficient of recharge is 5.0-6.0%.

4.7. Semipermeable Unit (AG-3)

The Semipermeable unit is started with thin-bedded shale of Lower Lutecian, which is interbedded with sandstone, conglomerate, and micritic limestone. Shale is impermeable, but sandstone, conglomerate, and limestone units have well-developed fracture and joint systems with increased secondary porosity and permeability. At the contact of shale and sandstone, small discharging springs are present. Some low discharging springs are related to faults and fracture systems. The upper layers of this unit are composed of volcanic breccias of Upper Lutecian. Within breccia, the andesitic lava flows are also present, which is compact and fractured. The drainage system is deep dendritic. The precipitation is the only source of recharge and the estimated coefficient of recharge is 4.0-5.0%.

4.8. Permeable Unit (Qal)

The Niksar Valley fill materials have started from the base with clayey-sandy gravels, loosely cemented sandstones, and

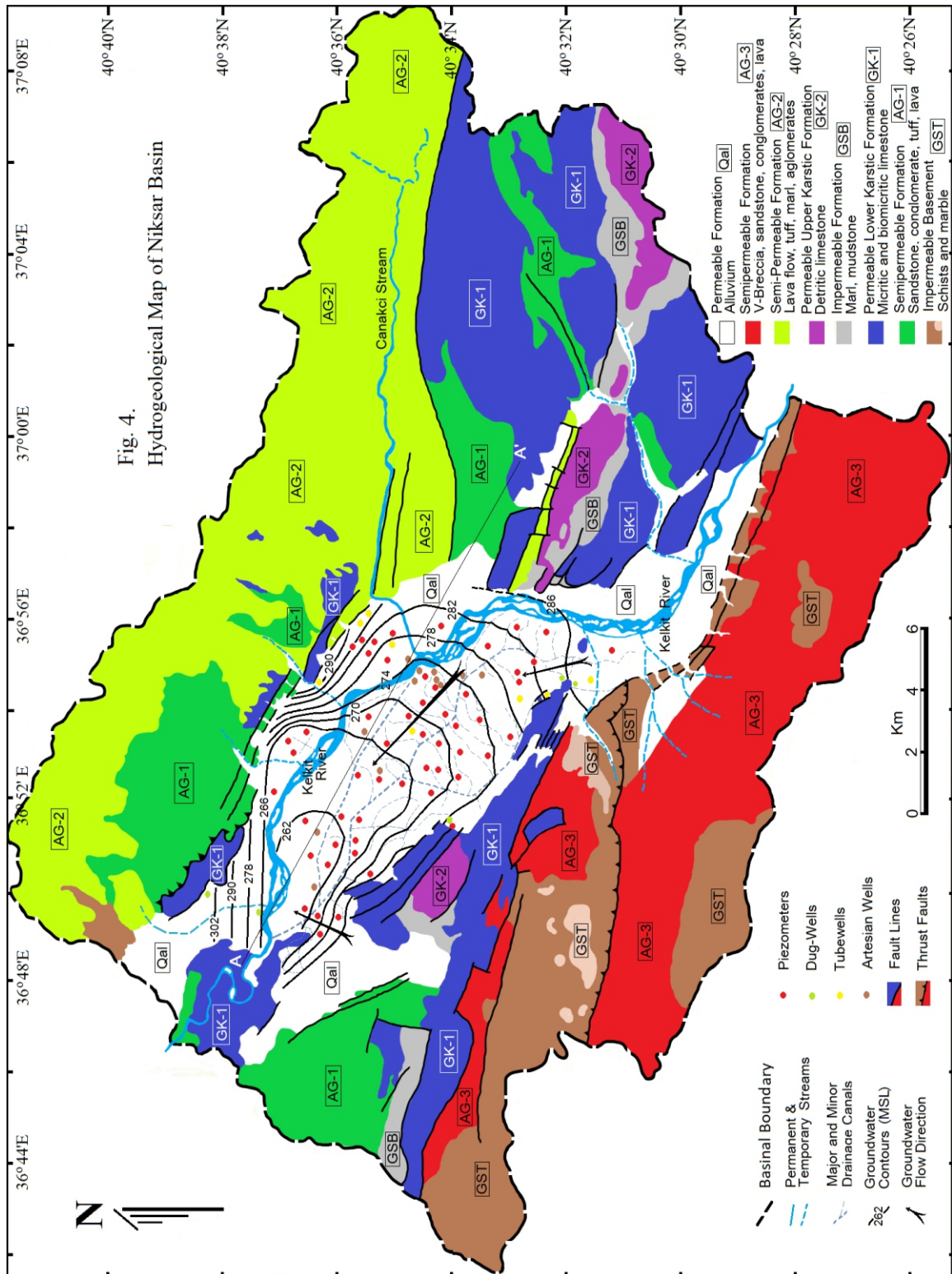
conglomerates of the Pliocene. These sediments are cropped out in the North-Western part of Niksar town. The gravels are well-rounded and poorly sorted. The unit is largely composed of large clastic materials of the Pliocene, at some places small size particles are exceeded. The lithological logs of drilling wells and the geophysical studies represent that the Pliocene sediments are hundreds of meters thick. These sediments are overlain by a 25-70m thick alluvium sheet. These sediments have an aquifer of high yield; in the Northern and Southern slopes of Niksar Valley, a series of small and large alluvium cones are present. The alluvium aquifer recharges directly from precipitation, Kelkit River, flood irrigation, and perennial streams. The coefficient of recharge by precipitation is 30% and surface flows are 5%. The groundwater from the alluvial aquifer is drawn by digging wells, hand pumps, and drilled wells. The deepest well drilled in the valley is 240m. In Niksar Valley fill material after an average depth of 40m the gravel formation of Pliocene starts. The gravel, sand, and clay beds are of varying thickness, color, particle size, and lithology. In between alluvial sediments, 2-23m thick a sheet of plastic clay is present. In the presence of the plastic clay layer, the alluvial aquifer is divided into a free surface and an artesian aquifer. In the Western part of Niksar Valley, the clay layer is thick and near to the surface while towards the East thickness gradually decreases and deep from the surface. The sediments above the clay bed have a greater thickness towards the east.

5. Recharge and Discharge of Hydrogeological Units

In the study area, eight hydrogeological formations are exposed, almost all formations are naturally recharged through precipitation. These hydrogeological formations are discharged by natural groundwater through small to large springs. For the study period, the recharge through precipitation for each unit is calculated with the following relationship; $I = A \times P \times I_e$. Where I is recharge through precipitation (m^3), A is the area of hydrogeologic units (m^2), P is precipitation (m), and I_e is coefficient of recharge (%). The coefficient of recharge varies from 0.01 to 0.40 depending on the lithological variations and primary and secondary porosity and

permeability of the hydrogeological units. The exposed hydrogeological units covering an area of 655 km², the individual units range in area from 15 to 141 Km². During the study period, these units' recharge amount with precipitation varies from 0.001-0.265x10⁹m³. During the same period, the discharge amount varies from 0.001-0.263x10⁹m³. During the study

period, the total amount of recharge was $0.329 \times 10^9 \text{ m}^3$, and discharge was $0.317 \times 10^9 \text{ m}^3$. The difference of $0.012 \times 10^9 \text{ m}^3$ between total recharge and discharge quantities of all the hydrogeological formations is due to the average values, not considering the base flow of minor creeks, and evapotranspiration, Table 2.



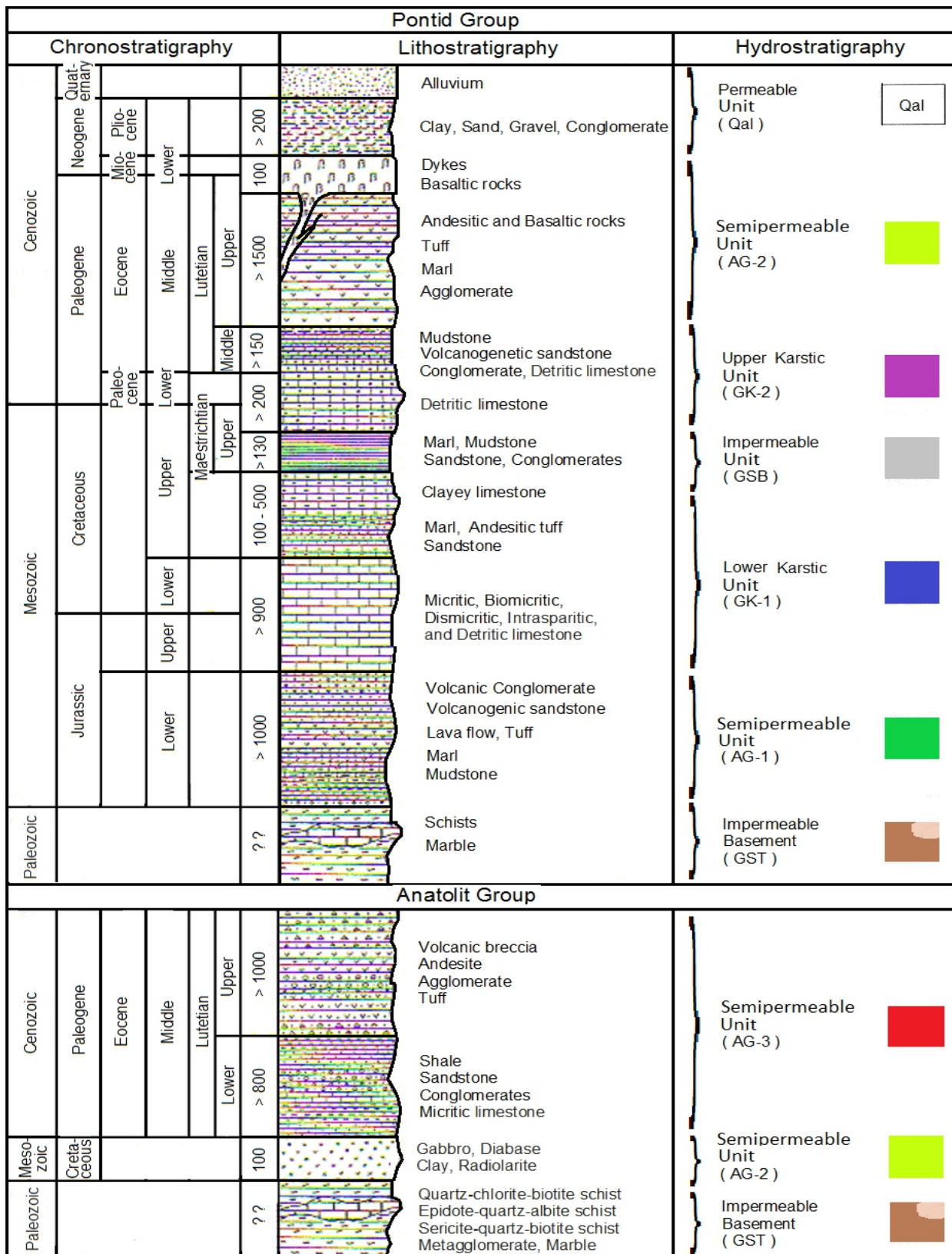


Fig. 5. Stratigraphic column of Niksar Basin showing the correlation between age, thickness, stratigraphy, lithology, and hydrogeologic units.

6. Hydrogeological Properties of Aquifers

In the study area, the free surface and artesian aquifers are developed in Quaternary Alluvium and loose sediments of the Pliocene. The general gradation trend of alluvial sediments has ranged from good to normal and the particles are different in size. The gradation of Pliocene sediments ranges from good to poor and has great variation in particle diameter and size distribution. The open space of filters used in installed tubewells in Niksar valley ranged from 0.5-2.0mm (d₄₀) as per intercepted formations, Table 3. The porosity, hydraulic conductivity (K), transmissivity (T), and storage coefficient were calculated in the lab with aquifer sediment samples and in the field by pumping and injection or slug tests. The secondary porosity is well developed in almost all the exposed formations, which is related to fractures, joints, cracks, bedding planes, and faults. The solution cavities in limestone formations play a dominant role in secondary

porosity. The pressing method of Castany (1963) was used to calculate the porosity of Quaternary loose sediments deposited by the Kelkit River and Pliocene sediments. The samples were collected from a depth of 3-4 m, the porosity values are given in Table 3. The porous box method of Schoeller (1967), utilized to calculate the permeability of Quaternary sediments. The constant head permeameter was utilized to calculate the permeability of Pliocene sediments. The pumping tests were conducted to calculate the T and K values by Theis (1935) and, Jacob (1947) methods, and the aquifer recovery test was analyzed by assumptions of Houpert-Pouchan; de Marsily, (1986), is presented in Table 4. The reserve constant and the effective radius of the pumping wells were not calculated due to the absence of piezometers. The Slug Tests were conducted in 13 shallow auger-hole wells to calculate the T, K, and storativity (S) values, (Bower, 1989). The results of the slug tests are presented in Table 5.

Table 2. Recharge and discharge quantities of hydrogeological units.

Hydrogeological Formations	Area (km ²)	Coefficient of Recharge (%)	Recharge (10 ⁹ m ³)	Discharge (10 ⁹ m ³)
Permeable Unit (Qal)	141	0.40	0.265	0.263
Semipermeable (AG-3)	121	0.05	0.005	0.003
Semipermeable (AG-2)	134	0.05	0.006	0.002
Permeable Upper Karstic (GK-2)	16	0.40	0.006	0.009
Impermeable (GSB)	15	0.01	0.001	0.001
Permeable Lower Karstic (GK-1)	108	0.40	0.043	0.036
Semipermeable (AG-1)	61	0.04	0.002	0.002
Impermeable Basement (GST)	59	0.01	0.001	0.001
Total	655	-	0.329	0.317

Table 3. Grain size, porosity, and permeability of hydrogeological units.

Hydro-geological Units	Grain Size				Porosity (%)		Permeability (m/s)					
	Uniformity Coefficient		Curvature Coefficient		Castany		Constant-Head Permeameter		Schoeller Method		Average	
	Min	Max	Min	Max	Min	Max	Min	Max	Min	Max		
Alluvium	7.1	30.1	1.9	3.0	16	35	1.8 x 10 ⁻⁴	1.4 x 10 ⁻⁶	2.4 x 10 ⁻⁴	2.7 x 10 ⁻⁶	1.1 x 10 ⁻⁴	
Sandy gravel	-	-	-	-	-	-	1.1 x 10 ⁻³	6.7 x 10 ⁻³	1.0 x 10 ⁻⁴	7.1 x 10 ⁻⁴	2.2 x 10 ⁻³	
Pliocene sediments	6.1	25.0	1.6	3.9	20	40	1.4 x 10 ⁻⁴	2.6 x 10 ⁻⁵	1.3 x 10 ⁻⁴	4.3 x 10 ⁻⁵	8.4 x 10 ⁻⁵	

Table 4. Results of well-pumping test analysis.

Well #	Water Bearing Formations	Theis		Jacob		Recovery	
		T (m ² /s)	K (m/s)	T (m ² /s)	K (m/s)	T (m ² /s)	K (m/s)
27267	Pliocene	5.2x10 ⁻⁵	3.0x10 ⁻⁶	5.4x10 ⁻⁵	3.2x10 ⁻⁶	9.0x10 ⁻⁵	5.3x10 ⁻⁶
27291	Alluvium	1.4x10 ⁻³	1.0x10 ⁻⁴	1.1x10 ⁻³	7.9x10 ⁻⁵	-	-
20588	Alluvium	3.2x10 ⁻²	2.1x10 ⁻³	7.2x10 ⁻²	4.8x10 ⁻³	-	-
20159	Alluvium	1.35x10 ⁻³	7.5x10 ⁻⁵	4.8x10 ⁻³	2.6x10 ⁻⁴	-	-
20159	Alluvium	1.34x10 ⁻³	7.4x10 ⁻⁵	2.3x10 ⁻³	1.3x10 ⁻⁴	7.9x10 ⁻³	4.4x10 ⁻⁴
20158	Alluvium	5.3x10 ⁻³	4.4x10 ⁻⁴	5.9x10 ⁻³	4.9x10 ⁻⁴	-	-
4985	Pliocene	2.6x10 ⁻⁴	5.3x10 ⁻⁶	5.1x10 ⁻⁴	1.0x10 ⁻⁵	-	-
4136	Pliocene	1.4x10 ⁻³	1.3x10 ⁻⁵	4.3x10 ⁻³	4.1x10 ⁻⁵	-	-
4684	Limestone	1.74x10 ⁻³	-	-	-	-	-
SK-2	Limestone	-	5.2x10 ⁻⁵	-	-	-	-
SK-3	Limestone	-	5.2x10 ⁻⁵	-	-	-	-

Table 5. Results of slug test analysis.

Well #	T (m ² /s)	K (m/s)	S
64	1.1x10 ⁻⁵	9.17x10 ⁻⁶	5.6x10 ⁻⁴
65	5.2x10 ⁻⁶	3.4x10 ⁻⁶	5.6x10 ⁻³
66	9.0x10 ⁻⁵	5.2x10 ⁻⁵	2.5x10 ⁻³
67	4.0x10 ⁻⁶	3.5x10 ⁻⁶	2.5x10 ⁻⁵
68	6.9x10 ⁻⁶	3.1x10 ⁻⁶	2.5x10 ⁻²
69	3.0x10 ⁻⁵	1.1x10 ⁻⁵	3.6x10 ⁻⁴
70	3.1x10 ⁻⁵	2.1x10 ⁻⁵	2.2x10 ⁻³
71	1.3x10 ⁻⁶	7.8x10 ⁻⁷	5.6x10 ⁻³
72	3.0x10 ⁻⁵	1.5x10 ⁻⁵	2.5x10 ⁻³
73	3.3x10 ⁻⁶	2.1x10 ⁻⁶	3.6x10 ⁻³
74	2.4x10 ⁻⁵	1.7x10 ⁻⁵	2.5x10 ⁻⁴
75	3.2x10 ⁻⁵	1.9x10 ⁻⁵	2.5x10 ⁻²
76	3.9x10 ⁻⁵	1.4x10 ⁻⁵	3.6x10 ⁻²

7. Hydraulic Head Conditions

To monitor the fluctuations in the groundwater table a network of 95 groundwater measuring points was established in the basin, Table 6. Continuous monitoring with a fixed interval of 5-10 days has been carried out. The major hydrologic factors which affect the short and long-term fluctuation of groundwater levels are precipitation, surface runoff, irrigation water, pumpage from wells, evaporation, transpiration, and discharge from

the artificial drainage canal system. The fluctuation caused by precipitation varies from place to place depends on topography, the thickness of the vadose zone, hydraulic conductivity, distance from permeable and impermeable boundaries, and structural elements including faults, fractures, folds, bedding planes, dip, strikes, and lithology of formations. In the Northern part of the Kelkit River, the groundwater level falls from February-April, and from August-October the groundwater reached its maximum level, the

the water level fluctuation is related to precipitation. In the Southern part of Kelkit River, the minimum water level was observed during the months of November-January and maximum during May-July. The groundwater level fluctuates under the influence of the flow level of the Kelkit River. The wells drilled in Upper Jurassic-Lower Cretaceous limestone formations represent a groundwater level rises and fall quite rapidly. The eight-meter variations in groundwater level are due to a well-developed karstic system. In the central part of the aquifer, the groundwater level fluctuations represent an irregular pattern. In the said area the precipitation, irrigation water, evapotranspiration, and flow through artificial drainage canals affect the groundwater levels. Comparison between precipitation, Kelkit River flow, discharge of artesian well, and groundwater level fluctuations are presented in Figure 3. The groundwater table is 0-2m deep in an area of about 50 km² at the central part of the basin, Figure 5. The General Directorate of State Hydraulic Works of Turkey maintaining a drainage system of two-meter-deep to control the water table in the valley (DSI,1968-1988). The drainage system is comprised of main and subsidiary surface drainage canals. The water level fluctuates in the drainage canals have a similar pattern with the water level of Kelkit River. The minimum and maximum discharge from drainage canals was 3.21 and 6.15m³/s observed on October 2, 1986, and October 13, 1987, respectively. The Total discharge from drainage canals for the budget period was 129.9x10⁶m³.

The maximum rise in the water table of the unconfined aquifer was observed in June 1987 and the minimum water level in December 1986. The hydraulic gradient is different from region to region and ranged from 1.6x10⁻³ to 2.5x10⁻². The difference in water level ranged from 0.01-9.4m. The artesian wells present in the central part of the Niksar Basin toward the western side of the Kelkit River. The hydraulic head variation of confined aquifer measured from artesian wells, the potentiometric surface varies from 0.02-0.40m above the ground surface of the valley. The potentiometric levels vary with the variation in precipitation and water level of the Kelkit River. The potentiometric surface represents a similar

pattern of fluctuation in all parts of the confined aquifer, the maximum and minimum level observed in May and March respectively. The hydraulic gradient of the potentiometric surface in June 1987 was 1.2 x10⁻³ to 6.5x10⁻⁴. The surface and groundwater interaction via a comparison between precipitations, discharge of streams, drainage canals, artesian well, and groundwater level fluctuations in the alluvium wells are presented in Figure 3.

8. Groundwater Table Maps

Niksar Valley is comprised of confined and unconfined aquifer systems developed under suitable hydrodynamic conditions. The water table maps of the unconfined aquifer and potentiometric surface of the confined aquifers were prepared for the highest and lowest periods of the water table. The water table map of the unconfined aquifer was prepared with the help of 85 monitoring points; among them, 13 are dug wells, 63 piezometers, 9 drilled wells, and 10 artesian wells. The highest level of groundwater table for unconfined aquifer was prepared for June 1987, Figure 6a. Kelkit River and drainage canals affect the groundwater levels and flow directions. The dominant groundwater flow direction is towards NW. The Kelkit River round the year feeds the aquifer from the eastern side. While from the western side round the year, the drainage canals and unconfined aquifer directly feed the Kelkit River. The groundwater flow direction and the hydraulic gradient is diverse from place to place in the valley. The hydraulic gradient ranges between 2.0-3.0x10⁻³.

The lowest period groundwater table map of the unconfined aquifer was prepared for December 1987, presented in Figure 6b. It represents that the general groundwater flow direction is almost the same everywhere as in the maximum level groundwater map. The equal groundwater flow contour lines become wider. The minimum and maximum groundwater levels fall from 3.8-9.4m. The groundwater level of the unconfined aquifer was highest in June 1987 and lowest during December 1986. Based on the difference of both levels, the equal change in groundwater level map prepared, Figure 6c. The monitored minimum difference in both levels was 0.01m at piezometer No. 61.

The maximum difference was recorded at 9.4m at drilled well No. 4684. The groundwater level change in the western and central parts of the valley is less than 1.0m. From the east towards the northern and southern parts, the difference in groundwater level is 1-4m. Towards the east, it varies from 4.0-7.0m and further east it's more than 9.0m.

The Quaternary and Pliocene deposits are predominantly recharged by the Kelkit River rather than precipitation. The alluvium naturally discharges to the Kelkit River and artificial discharge took place through drainage canals and pumping wells. The aquifer recharged with different sources during the study period. The difference in maximum and minimum groundwater table maps between June 1987 and December 1986 was calculated with the relationship; $V = S \times A \times \Delta h$, and $\Sigma V = V_1 + V_2 + V_3 + V_4$. Where V is the aquifer's recharge volume in m³. A is an area of equal change in water level m², Δh is the equal change in quantity m. The n is porosity, an average of 30%. V_1, V_2, V_3, V_4 , are equal water changed in different areas of the aquifer in m³. The difference in groundwater level during the lowest and highest periods of study ranges from 0 to >7m. The equal change in groundwater level at region $h_1 = 0 - 1$ m, $h_2 = 1 - 4$ m, $h_3 = 4 - 7$ m and $h_4 = > 7$ m, Figure 6c. The calculated volume of equal change in water level at different areas of the aquifer are as follows; $V_1 = 0.019 \times 10^9$ m³; $V_2 = 0.022 \times 10^9$ m³; $V_3 = 0.019 \times 10^9$ m³; and $V_4 = 0.079 \times 10^9$ m³.

The total volume of water recharged to the aquifer during the study period was $V = 0.139 \times 10^9$ m³. For the study period, equal change in the groundwater table map is prepared by the values of the difference between the two lowest periods of the unconfined aquifer of the valley. The groundwater table equal change map based on a difference in values of December 1986 and February 1988, Figure 6d. The groundwater table was high in February 1988 as compared to December 1986, the rise varies between 0-2 m in different parts of the valley. During the same time, the total groundwater addition (Δs) in the aquifer was 0.054×10^9 m³.

Ten artesian wells existed in the valley drilled by DSI. The piezometric surface maps of the confined aquifer developed in the valley were drawn with the help of artesian wells. The discharge of the artesian wells and piezometric surface regularly monitored during the study period for correlation, presented in Figure 3. The highest piezometric surface level map for June 1987 has been prepared, shown in Figure 7a. The piezometric surface contour lines are very smooth and parallel to each other and increasing from Northward to Southward. The lowest piezometric surface level of the confined aquifer was observed in December 1986, the map is presented in Figure 7b. The groundwater flow direction of the confined aquifer and pattern of the piezometric contour lines remains the same during both the highest and lowest periods. The groundwater flow direction also remains the same from Southward to Northward parallel to the flow of Kelkit River. The difference in the highest and lowest period of piezometric surfaces varies between 1.10-2.20m observed at drilled artesian well numbers 86 and 1611. The hydraulic gradient of the piezometric surface during 1987 in the eastern region ranges from 1.2×10^{-3} to 6.5×10^{-4} , and in the western region increased to 2.4×10^{-3} .

9. Karstification and Karstic Springs

The Jurassic-Cretaceous limestone formations have a well-developed karstic system in the area. Interconnected diffused and conduit flow system developed together in karstic limestones. The karstification, groundwater movement, recharge, and discharge studies were conducted, (Aftab et al., 1997). The groundwater movement mainly depends on variation in lithology and hydraulic properties. The lateral extent of the recharge area is quite significant, and precipitation is the only source of recharge. The units discharge through several small to large karstic springs. The infiltration rate has varied, from place to place depending upon structure, topography, soil cover, and solution cavities. To analyze the karstification process, geochemical analysis of a few rock samples from different localities was analyzed, (Taskin, 1977). The analysis represents that despite all lithological variations the CaO quantities vary between

49.3-55.6%. While the CaCO₃ quantity in all samples ranges from 88.0-99.3%. The analysis represents that the excessive amount of CaCO₃ in limestone formations helps to react fast with

rich carbonic acid rainwater to dissolve and wider solution cavities. It's technically confirmed that in well-developed karstic regions, the CaCO₃ is more than 90%.

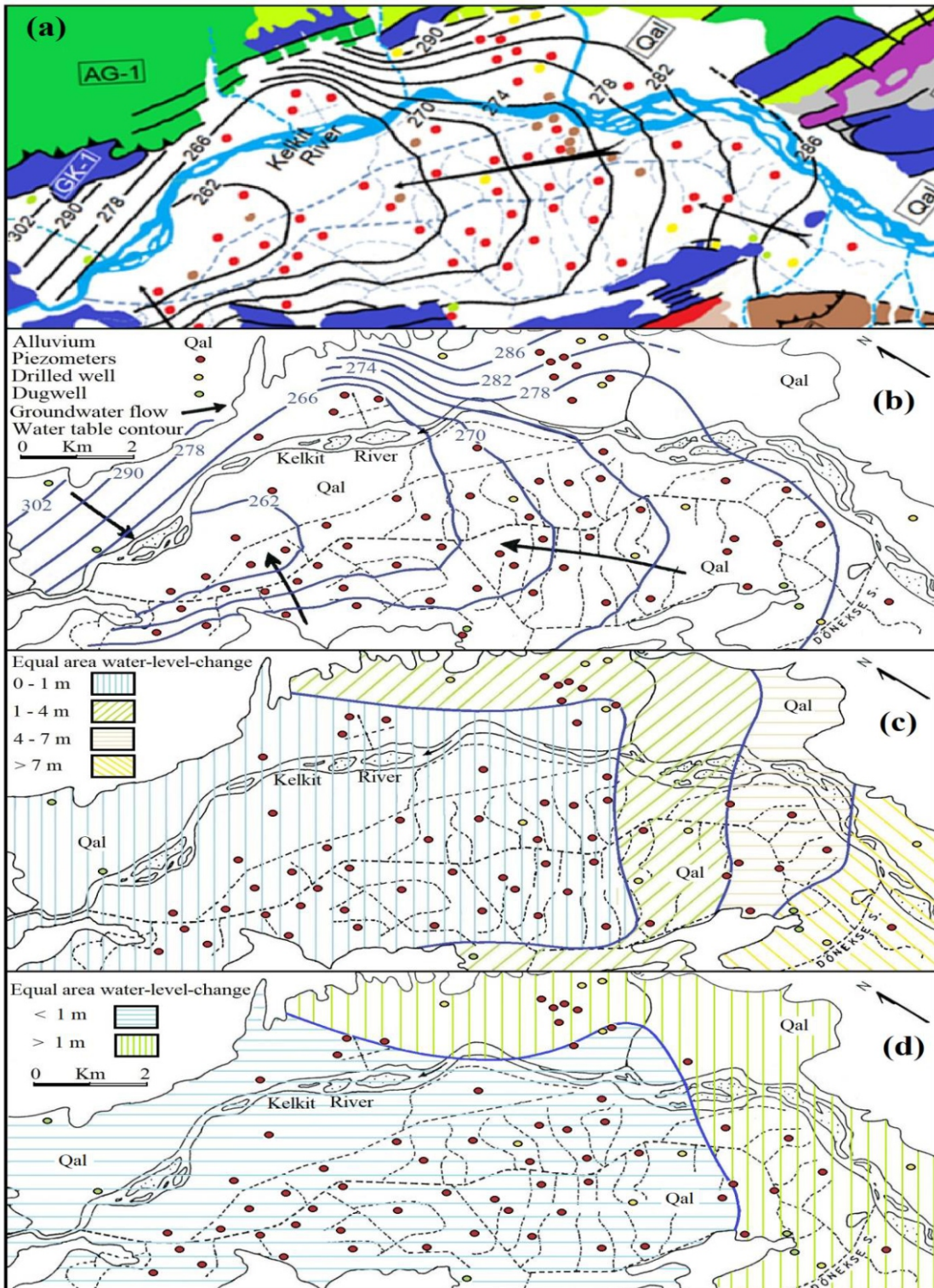


Fig. 6. Groundwater table contour maps of unconfined aquifer (masl); a) highest level contour map of June 1987, b) lowest level contour map at December 1986, c) groundwater-level-change-map between highest and lowest levels, d) groundwater-level-change-map between two lowest levels December 1986 and February 1988; for legend see Figure 5.

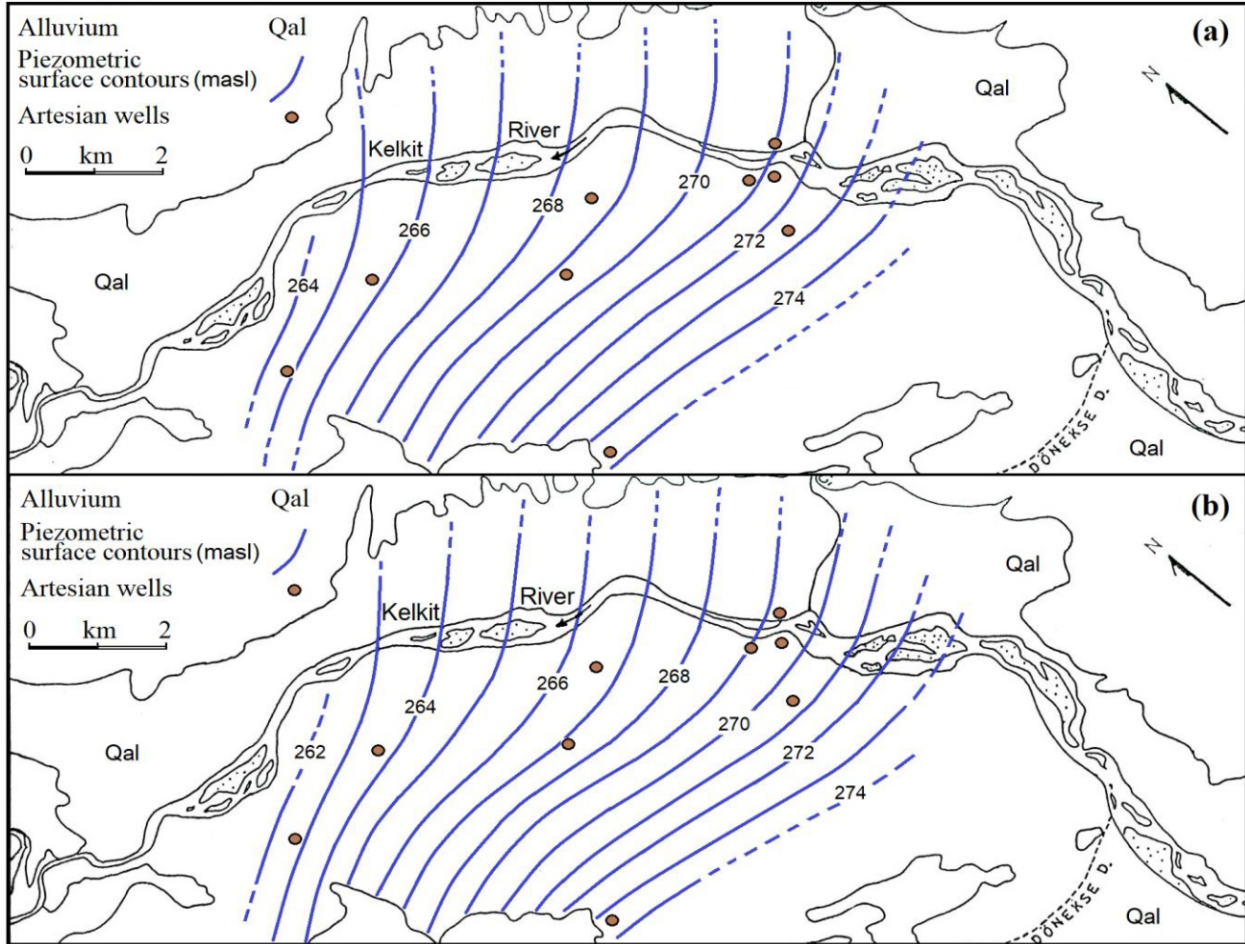


Fig. 7. Potentiometric surface maps of confined aquifer; a) during highest level potentiometric surface map June 1987; b) lowest level potentiometric surface map December 1986.

Several karstic and non-karstic springs emerge from karstic and hard rocks located in the study area. The inventory and monitoring of 51 springs having a discharge of more than 1.0 L/s were conducted during the study period. The karstic springs of low to high discharge are emerging from limestone formations of Jurassic-Lower Cretaceous, Upper Cretaceous, and from Upper Cretaceous-Lower Paleocene. The discharge of the karstic springs varies from 1.0-500 L/s. Many other small springs are emerging from different geological formations with a variation in discharge from 0.5-5.0 L/s. The majority of these springs are originating through faults and are classified as fault springs. The andesitic and basaltic formations of Eocene are severely fractured and faulted from where emerging springs are fracture springs. The small springs emerge from bedding planes and formation contacts of Paleozoic schists comprised of sedimentary series and mudstone of Upper Cretaceous, and flysh series of Eocene. The valley springs

emerge in depressions and major artificial drainage canals. The geological cross-section and weekly discharge hydrographs of nine major karstic springs were analyzed systematically. The discharge coefficient, reserve capacity, and discharge volume were evaluated by Castany's relationship, (Castany, 1963). $q = q_0 e^{-\alpha(t-t_0)}$, where $q = t$ times discharge in m³/s, q_0 = to times discharge or start at reserve discharge in m³/s. $e = 2.718$ or $\ln = 0.434$, α = discharge coefficient in days. The reserve estimation of karstic springs above the point of discharge, discharge coefficient, the volume of the potential reserve or reserve capacity (V) calculated with the Maillet integration as follows (Maillet, 1905);

$$V = \int_{t_0}^{\infty} q \cdot dt \quad \text{or} \quad V = \frac{q_0}{\alpha} 86400$$

In the equation t_0 and t used to calculate the difference of total spring discharge. Yolkonak-II spring in one of the largest springs

originates at the contact of valley alluvium and Permeable Lower Karstic Unit (GK-1). The unit is comprised of Jurassic to Cretaceous age formations composed of biomicritic, dismicritic, and intrasparite limestone having a well-developed karst system. Two recession periods encountered during the study period, in both hydrodynamic regimes of karst aquifers were analyzed. The first discharge regime of spring comprised of 145 days and discharge varies between $q_0 = 240 \text{ L/s}$ to $q_1 = 68$. During the same regime discharge coefficient $\alpha = 0.00874 \text{ day}^{-1}$, the actual discharge was $q = q_0 e^{-0.0087t}$, reserve's storage capacity $V = 1.7 \times 10^6 \text{ m}^3$. The second real discharge regime of the same spring comprised 115 days, whereby $q_0 = 445 \text{ L/s}$ and $q_2 = 17 \text{ L/s}$. The discharge coefficient $\alpha = 0.0085 \text{ day}^{-1}$, and the actual discharge was $q = q_0 e^{-0.0085t}$. During

this regime, the spring's storage capacity $V = 2.79 \times 10^6 \text{ m}^3$. The total spring discharge volume during the entire study period was $8.61 \times 10^6 \text{ m}^3$, this quantity is the sum of discharges of two actual discharge regimes and an increase in flow due to recharges. Yolkonak-II Spring analysis, schematic geological x-section, origin, recession curves dynamics, and discharge hydrograph is presented in Figure 8. The minimum to the maximum discharge of nine major karstic springs ranges from 4.3 to 430 L/s , discharge coefficient from 0.0009 to 0.0255 day^{-1} , storage capacity from 0.14 to $5.01 \times 10^6 \text{ m}^3$, and discharge volume varies from 0.27 to $8.61 \times 10^6 \text{ m}^3$. During the study period, the total storage capacity and discharge volume of all nine springs were 14.78 and $48.08 \times 10^6 \text{ m}^3$ respectively. The hydraulic properties of springs are given in Table 6.

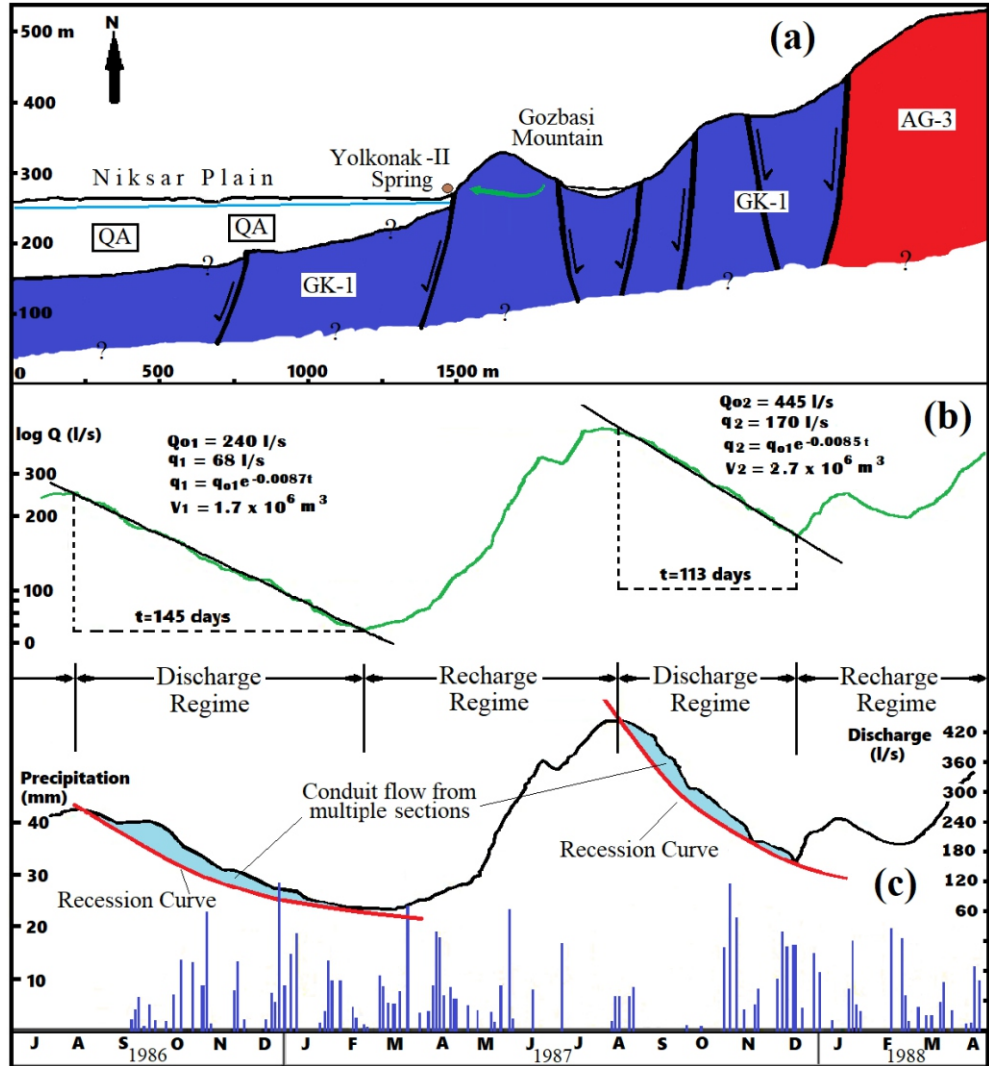


Fig. 8. Yolkonak-II Spring analysis; a) geological x-section, b) recession curves dynamics, c) discharge hydrograph; for legend see Figure 5.

10. Groundwater Budget

The groundwater budget for the Quaternary and Pliocene aquifer spread over an area of 141 Km² were appraised, (Canik, and Aftab, (1990). The groundwater budget for the period of October 1986 to September 1987 was calculated by measuring all elements of recharge and discharge to and from an unconfined aquifer. To calculate the groundwater budget general budget equation of Schoeller, and Canik was utilized (Schoeller, 1967; and Canik, 1971). The groundwater budget equation in its simplest form may be written as;

$$P + V'r_1 + V'r_2 + V'n + V'a = Etr + Vr + Vnr + \Delta s + Va_1 + Va_2$$

Where P= Precipitation, V'r₁= Recharge from Kelkit river, V'r₂ = Recharge from Canakci stream, V'n = Recharge from other aquifers, V'a = Recharge from irrigation waters, Etr = Evapotranspiration, Vr = Surface runoff, Vnr = Discharge to Kelkit river, Δs = Addition in the aquifer reserve, Va₁ = Discharge by drainage canals, Va₂ = Water withdrawal from the aquifer by pumpage. During the budget period, the aquifer received a maximum quantity of water from the Kelkit River which is 0.171x10⁹m³ and 64.3% of all recharge quantities. Aquifer discharge maximum quantity through drainage canals 0.125x10⁹m³ which is 47.5% of total discharges. The aquifer received a total quantity of 0.266x10⁹m³ of water and discharged 0.263x10⁹m³ of water through all sources. The difference of 0.003x10⁹m³ is due to average values of recharge and discharge parameters measuring errors, and unmeasured parameters, etc. The recharge and discharge elements along-with percentage values are presented in Figure 9.

11. Conceptual Hydrogeological Model

The detailed regional-scale hydrogeological and groundwater investigations of Niksar Basin represent a complex hydrogeological system. The significance of topography, geology, and tectonics of the area premeditated and correlated with the regional flow parameters of the study area. The conceptual model is based

on hydrogeological parameters prepared with realistic field conditions of Niksar Valley. The model signifies hydroclimatic, hydrogeomorphologic, hydrostratigraphic, hydrogeological, and hydrologic data to define the physical parameters of water-bearing formations, (Aftab, 2017a, b). The model-oriented northwest-southeast direction along the cross-sections A-B of the hydrogeological map of the Niksar Basin Figure 5, and enlarged along cross-section X-Y. The model represents geological, lithological, tectonic, and climatical descriptions along-with surface and subsurface hydrogeologic components of confined and unconfined aquifers, Figure 10. The important input parameters of the model are temperature, precipitation, humidity, thermal index, wind speed, and direction with associated groundwater recharge. The parameters related to land cover are topsoil depth, porosity, hydraulic conductivity, and residual water content. These parameters are important for infiltration and groundwater movement. The model also represents hydraulic-head conditions, aquifer storability, transmissivity, and hydraulic conductivity. The actual evapotranspiration, surface runoff, subsurface flow, and groundwater discharge among different sources are resulting parameters. The conceptual model represents all physical processes observed through field investigations.

The conceptual hydrogeological model of Niksar Basin maybe translates into a GIS-based three-dimensional calibrated numerical groundwater flow model of the basin. By incorporating published and unpublished additional study data, the model may interpolate geological and tectonic relationships with the flow system of basinal aquifers. The model may have utilized in the future for decision support and studies on the impact of climate change on groundwater balance in time and space. The climatical effects on karstification processes and the flow patterns of Niksar Karstic springs may also interpolate and envision.

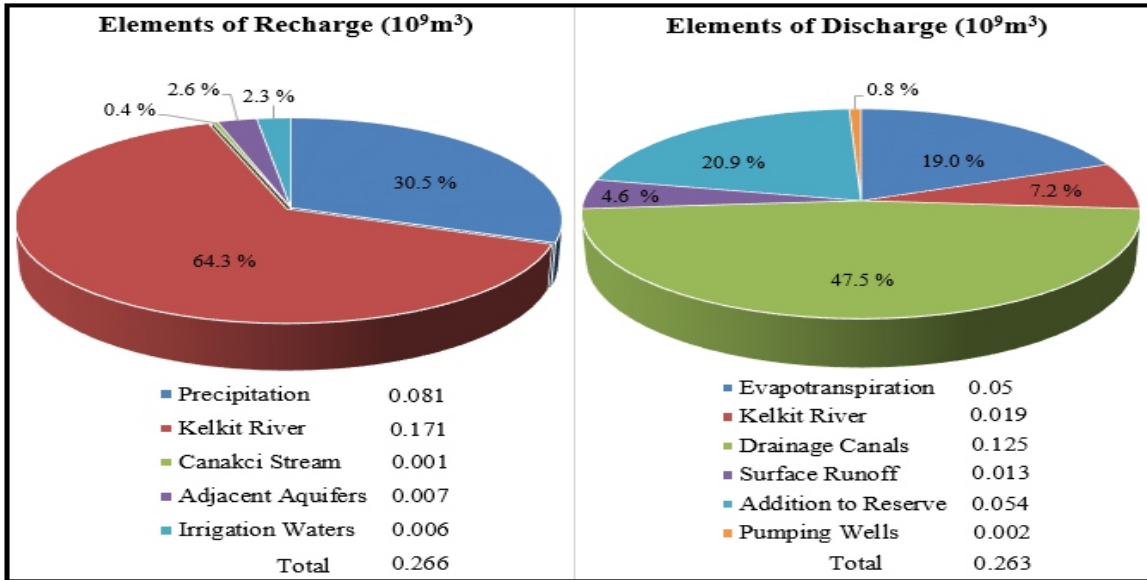


Fig. 9. Recharge and discharge elements of groundwater budget of Quaternary Aquifer.

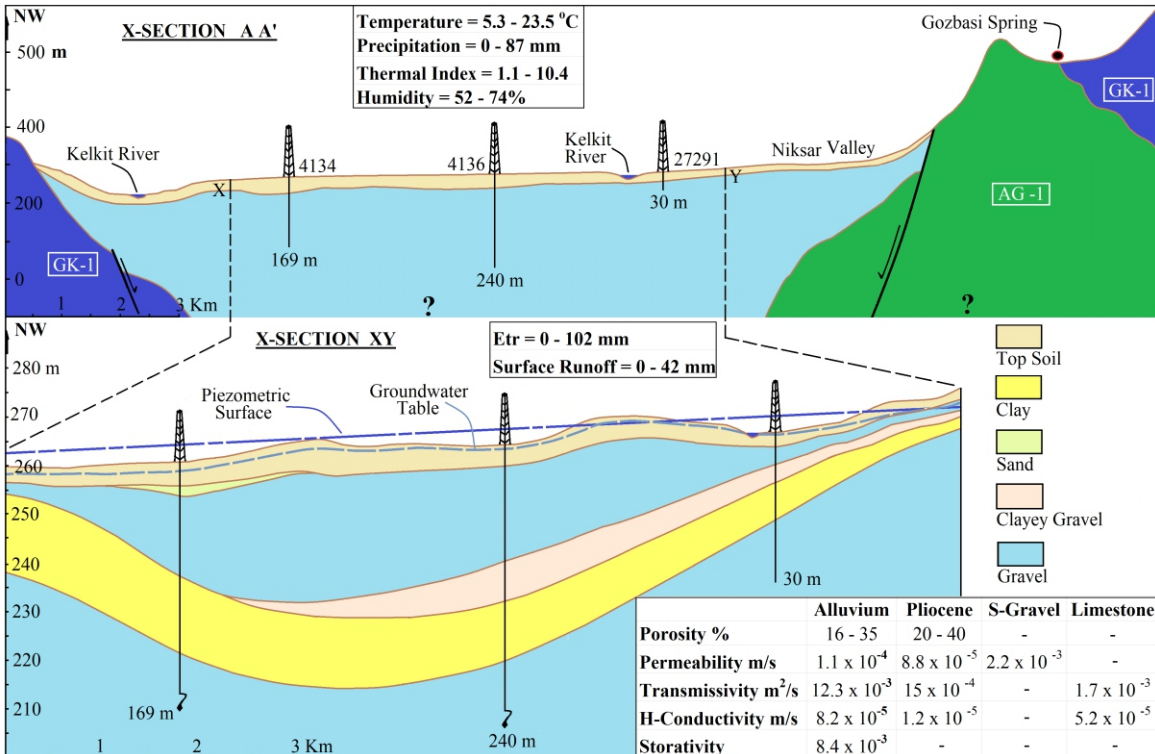


Fig. 10. Conceptual hydrogeological model of Niksar Valley; for legend see Figure 5.

11. Conclusion

The Paleozoic Schists from an impermeable basement in the study area, while the isles of marble form permeable zones. The limestone formations of Upper Jurassic-Lower Cretaceous and Upper Maastrichtian-Lower Paleocene form important karstic aquifers GK-1 and GK-2 respectively. The marl and mudstone of Upper Maastrichtian form significant impermeable boundaries GSB

among geological formations. The average yearly precipitation 551mm, Etpc 742mm, Etr 357mm, water deficit 384mm, and water surplus 194mm. About 65% of precipitation return back to the atmosphere through evapotranspiration. The soil moisture recharge was 35% of precipitation, the surface runoff is 28% of precipitation. The groundwater flow directions of confined and unconfined aquifers are different from region to region, but in the eastern and central regions, it's from southeast

to northwest. The hydraulic gradient of confined and unconfined aquifers are diverse from place to place and vary from season to season; ranges between 1.2×10^{-3} to 6.5×10^{-4} , and from 2.0 to 3.0×10^{-3} , respectively. Induced groundwater resources and the interaction between surface and groundwater-dominated by the flow of Kelkit River. Kelkit River discharged $5.57 \times 10^9 \text{ m}^3$, base flow $3.12 \times 10^6 \text{ m}^3$, Canakci Stream discharged $35.82 \times 10^6 \text{ m}^3$, base flow $11.48 \times 10^6 \text{ m}^3$, and discharged from artificial drainage canals $0.221 \times 10^9 \text{ m}^3$ of water. The eight hydrogeological formations that exposed on an area of 655 km^2 recharged through precipitation $0.329 \times 10^9 \text{ m}^3$ and discharged $0.317 \times 10^9 \text{ m}^3$ during the study period. The karstic formations recharged from precipitation $49.92 \times 10^6 \text{ m}^3$, while discharged from karstic springs $48.08 \times 10^6 \text{ m}^3$. The discharge coefficient of nine karstic springs ranges from 0.0043-0.01 day⁻¹, and storage capacity above discharging point varies from 0.14-5.0 $\times 10^6 \text{ m}^3$. The groundwater budget represents that aquifer recharged from different sources $0.266 \times 10^9 \text{ m}^3$ of water and discharged $0.263 \times 10^9 \text{ m}^3$ through all sources. The conceptual hydrogeological model of the Niksar Valley signifies hydroclimatic, hydrogeomorphologic, hydrostratigraphic, and hydrogeological field environments. The model characterizes geological, tectonic, climatical, surface, and subsurface hydrogeologic components of confined and unconfined aquifers.

Acknowledgment

The Higher Education Commission of Pakistan financed to present the study at the GSA Annual Meeting held on October 22-25, 2017 in Seattle, Washington, USA (Aftab, 2017a, b). This classical study is part of Ph.D. dissertation entitled, "Hydrogeological Investigations of Niksar (Tokat) Basin, Turkey" submitted to the Science Faculty of Ankara University, Turkey, (Aftab, 1989). The hydrogeological investigations were conducted under the supervision of late Professor Dr. Baki Canik. The purpose of this publication is to acknowledge the professional excellence of Professor Canik as a pioneer in the field of Hydrogeology.

Author's Contribution

Syed Mobasher Aftab conducted this research work as part of the Ph.D. dissertation entitled, "Hydrogeological Investigations of Niksar (Tokat) Basin, Turkey", submitted to the Department of Geological Engineering, Science Faculty, Ankara University, Turkey.

References

- Aftab, S M, 1989. Hydrogeological Investigations of Niksar (TOKAT), Valley, Turkey. Unpublished PhD Dissertation, (Turkish), Ankara University, Ankara, Turkey, pp.324.
- Aftab, S M, 2017a. Hydrogeology of Niksar Basin, Tokat, Turkey. GSA Annual Meeting in Seattle, Washington, USA - Paper No. 121-9, Abstract. Geological Society of America Abstracts with Programs. 49 (6) doi: 10.1130/abs/2017AM-29989,
- Aftab, S M, 2017b. Hydrogeology of Niksar Basin, Tokat, Turkey. GSA Annual Meeting in Seattle, Washington, USA - Paper No. 121-9. Presentation, Handouts PDF.
- Aftab, S M, AFSIN, M., and CELIK, M., 1997. Hydrogeological Study and Discharge Features of the Niksar Karst Springs, Turkey. The Arabian Journal for Science and Engineering. Dehran, Saudi Arabia. 22(2A), 131-144.
- Atkinson, T. C., Hydrol, J., 1977. Diffuse Flow and Conduit Flow in Limestone Terrain in Mendip Hills, Somerset, Great Britain, 35, 93-100.
- Blumenthal, M M., 1950. Orta ve Asagi Yesilirmak Bolgelerinin (Tokat, Amasya, Havza, Erbaa, Niksar) Jeolojisi Hakkinda. M.T.A. Seri D, No.4, (Turkish) Ankara, Turkey.
- Bouwer, H. H., 1989. The Bower and Rice slug test – An update. Ground Water, 27 (3), 304-309.
- Canik, B., 1971. Yeraltı Suya Rilaneosu, MTA dergisi No. 76, (Turkish), Ankara, Turkey.
- Canik, B., and Aftab S M., (1990). Groundwater Budget of Niksar (Tokat) Valley, Turkey. "Communication", Journal of Science Faculty of Ankara University, (Turkish), Turkey, 8, 1-11.
- Castany G., 1963. Traité pratique des eaux

- souterraines. Dunod, Paris, 657.
- De Marsily, Ghislain, 1986. Quantitative hydrogeology Groundwater hydrology for engineers: New York, Academic Press, Inc., pp. 440.
- De Martonne, E., 1942. Nouvelle carte mondiale de l'indice d'aridité. Annales de Géographie 51, 242–250 (in French).
- General Directorate of Electrical Affairs Etud Administration of Turkey (EIE), 1968-1988.The daily discharge rates data of Kelkit River.
- General Directorate of State Hydraulic Works of Turkey (DSI), and Ministry of Agriculture, Forestry General Directorate of Meteorology Affairs (DMI), 1968-1988. The monthly drainage, precipitation, temperature and wind speed at different meteorological stations in and around Niksar.
- Gunn, J., G. Gunay & A. I. Johnson, 1985. A Conceptual Model for Conduit Flow Dominated Karst Aquifers", in Karst Water Resources. Proc. Ankara Symp. IAHS, Publication, 161, 587-596.
- Jacob, C.E., 1947. Drawdown test to determine effective radius of artesian well, Trans. American Society of Civil Engineers, 112, , 1047-1064.
- Maillet, E., 1905. Essais d'hydraulique souterraine et fluviale. Librairie Sci., A. Hermann, Paris, 218.
- Schoeller H., 1967. Quantitative evaluation of groundwater resources. In: Methods and Techniques of Groundwater Investigation and Dev. UN Water Resources Series 33: pp. 21-44.
- Schoeller, H., 1962. Les eaux souterraines. Hydrologie dynamique et chimique; recharge, exploitation et evaluation des resources, 1, 642.
- Schoeller, H., 1967. Methods Pour Obtenir Le Bilan Des Eaux Souterrainex. Extrait de "Eaux Souterraines" Assemblee Generale de Berne, Louvain, Belgium.
- Seymen, I., 1975. 'The Tectonic Features of the North Anatolian Fault Zone in Kelkit Valley", Ph. D. Thesis, ITU Faculty of Mines, Istanbul, (Turkish), Turkey. pp. 192.
- TASKIN. C., 1977. Tokat ili Niksar ilce Merkezi cevresindeamento ve toz kirec hammade olanaklarinin arastirilmasi hakinda repor. M.T.A. Der. No. 6004. Ankara.
- Theis, C. V., 1935. The relation between the lowering of the piezometric surface and the rate and duration of discharge of a well using ground-water storage. Eos, Transactions American Geophysical Union, 16(2), 519-524.
- Thornthwaite, C. W., 1948. An approach toward a rational classification of climate. Geographical review, 38(1), 55-94.
- Turc, L., 1961. Water requirements assessment of irrigation, potential evapotranspiration: Simplified and updated climatic formula. Annales Agronomiques, 12, 13-49